Original Article

Morphological, Fractal, and Textural Features of the Mandible in Familial Mediterranean Fever Patients: A Case-control Study

Ailevi Akdeniz Ateşi Olan Hastalarda Mandibula'nın Morfolojik, Fraktal ve Dokusal Özellikleri: Olgu Kontrol Çalışması

Melek TASSOKER[1], Muhammet Üsame ÖZİÇ[2], Büşra ÖZTÜRK[1]

[1]Necmettin Erbakan University Faculty of Dentistry, Department of Oral and Maxillofacial Radiology, Konya, Türkiye
[2]Pamukkale University Faculty of Technology, Department of Biomedical Engineering, Denizli, Türkiye

ABSTRACT

Objective: Familial Mediterranean fever (FMF) is an inflammatory disease and chronic inflammation may affect bone turnover and metabolism. This study aimed to compare the morphological, fractal, and textural features of the mandibular bone in FMF patients with healthy controls on panoramic radiographs.

Methods: Fifty patients with FMF and, age- and sex-matched 50 healthy controls were included in the study. Morphological evaluation of the mandibular cortex on digital panoramic images of a total of 100 individuals was performed using the mandibular cortical index (MCI). For fractal dimension (FD) and texture analysis of trabecular bone, regions of interest with a size of 50x50 pixels were selected from the trabecular bone region between the roots of the second premolar and first molar teeth. The box-counting method was applied to calculate the FD. Since the pixel gray-scale levels of these regions showed different distributions, pre-processing was performed with histogram equalization for texture analysis. First-order and gray-level co-occurrence matrix-based second-order features of panoramic images were calculated and their textural characterizations were obtained.

Results: The MCI values of the mandibular cortex did not significantly differ between the case and control groups (p>0.05).

ÖZ

Amaç: Ailevi Akdeniz ateşi (FMF) inflamatuar bir hastalıktır ve kronik enflamasyon kemik döngüsünü ve metabolizmasını etkileyebilir. Bu çalışmanın amacı panoramik radyografiler üzerinde mandibular kemiğin morfolojik, fraktal ve dokusal özelliklerini FMF hastaları ve sağlıklı bireylerle karşılaştırmaktır.

Yöntemler: Çalışmaya FMF tanısı alan 50 hasta ve yaş ve cinsiyet açısından uyumlu 50 sağlıklı kontrol dahil edildi. Toplam 100 hastanın dijital panoramik görüntüleri üzerinde mandibular korteksin morfolojik değerlendirmesi mandibular kortikal indeks (MKI) kullanılarak yapıldı. Trabeküler kemiğe ait fraktal boyut (FB) ve doku analizi için, ikinci küçük azı ve birinci büyük azı dişlerinin kökleri arasındaki trabeküler kemik bölgesinden 50x50 piksel büyüklüğünde ilgi alanları seçildi. FB hesaplanmasında kutu sayma yöntemi uygulandı. Bu bölgelerin piksel gri-skala düzeyleri farklı dağılımlar gösterdiğinden doku analizi için histogram eşitleme ile ön işleme yapıldı. Panoramik görüntülerin birinci derece ve gri seviye eş oluşum matrisi tabanlı ikinci derece özellikleri hesaplanarak dokusal karakterizasyonları elde edildi.

Bulgular: Mandibular korteks MKI değerleri olgu ve kontrol grupları arasında anlamlı farklılık göstermedi (p>0,05). Trabeküler kemiğe ait FB değerleri olgu grubunda 1,43, kontrol grubunda 1,44

Cite this article as: Tassoker M, Öziç MÜ, Öztürk B. Morphological, Fractal, and Textural Features of the Mandible in Familial Mediterranean Fever Patients: A Case-control Study. Bezmialem Science 2024;12(2):246-55

*This study was presented as an oral presentation at the 2nd International Young Orad Symposium (March 5-9, 2024, Adana).

ABSTRACT

FD values for the trabecular bone were 1.43 in the case group and 1.44 in the control group, and there was no significant difference between them (p>0.05). First and second-order textural features of trabecular bone did not differ statistically significantly between the case and control groups (p>0.05).

Conclusion: Morphological, fractal, and textural features of the mandibular bone did not differ on panoramic radiographs between FMF patients and healthy controls.

Keywords: Familial Mediterranean fever, mandible, fractal, entropy, panoramic radiography

ÖZ

olup aralarında anlamlı fark yoktu (p>0,05). Trabeküler kemiğin birinci ve ikinci derece dokusal özellikleri olgu ve kontrol grupları arasında istatistiksel olarak anlamlı farklılık göstermedi (p>0,05).

Sonuç: Mandibular kemiğin morfolojik, fraktal ve dokusal özellikleri FMF hastalarında ve sağlıklı kontrollerde panoramik radyografiler üzerinde farklılık göstermemektedir.

Anahtar Sözcükler: Ailesel Akdeniz ateşi, mandibula, fraktal, entropi, panoramik radyografi

Introduction

Familial Mediterranean fever (FMF) is the most common autoinflammatory disease worldwide, characterized by self-limiting recurrent episodes of fever, polyserositis, and sometimes erysipelas-like dermatological findings (1,2). Populations of Mediterranean and Middle Eastern origin, such as Armenians, Greeks, Turks, Italians, and Arabs, are frequently affected by FMF (3). Symptoms appear in the first decade in 60-70% of cases and before the age of twenty in 80-90% (4). Thus, the majority of patients are diagnosed in the first two decades. FMF is caused by point mutations in the *MEFV* gene, which is located on the short arm of chromosome 16 and encodes the Pirin protein, and is inherited in an autosomal recessive manner (5). The frequency of the disease in Türkiye is approximately 1/1,000 and the carrier rate is 1:5 (6). Although the etiology is not fully understood, proinflammatory cytokines such as interleukin-6 (IL-6), IL-8, IL-12, and tumor necrosis factor-α (TNF-α) are elevated during FMF attacks (7). Colchicine treatment usually prevents attacks and inflammation (6).

Caries and periodontal diseases have been reported to be common in FMF (8). Temporomandibular joint arthritis associated with FMF is a rare maxillofacial finding (9) and recurrent aphthous ulcers may also be seen in these patients (8). Recurrent oral aphthous ulcers are rare mucocutaneous manifestations, may accompany attacks, and are thought to be related to dysregulation in cellular immunity, although the etiology is not clearly explained. Colchicine treatment has been reported to be effective on oral ulcers (8).

Methods such as mental index, gonial index, antegonial index, panoramic mandibular index, and mandibular cortical index (MCI) are used for radiographic evaluation of mandibular bone quality and density by examining panoramic radiographs, which are frequently used in dental practice (10). MCI, also known as Klemetti index (11), is more practical than other methods because it does not require any measurement. Scoring is done according to the degree of resorption in the mandibular cortex. Fractal analysis, a mathematical method, has been used frequently in recent years to analyze the complex structure of mandibular trabecular bone architecture. Its important advantages are that it is an easily accessible method, it is not affected by variables

such as projection geometry and radiodensity, and it provides objective data about the internal trabecular structure. As the fractal dimension (FD) increases, the complexity of the examined structure increases (12).

The texture is the repetition of a pattern or patterns over a region. These patterns may be fine, coarse, smooth, random, or striped in terms of quality (13). Disease-induced textural changes in radiological images of patients and normal control groups can be used as a marker for disease diagnosis. Statistical features can be obtained by using the cumulative and neighboring pixel behavior of grayscale-level pixel distributions in the regions of interest (ROI). For this purpose, first-order statistical (FOS) features and gray-level co-occurrence matrix (GLCM) based second-order statistical features are frequently used in the literature (14-17). FOS features calculate cumulative mean, variance, skewness, kurtosis, energy, and entropy values considering the grayscale-level color distribution in the histogram of the image (18). GLCM, on the other hand, can produce higher-quality features by considering the textural relationships arising from pixel neighborhoods. The GLCM defined by Haralick et al. (19) can calculate many statistical properties such as energy, correlation, entropy, homogeneity, and contrast, which can model texture changes according to pixel neighborhood orientation degree and pixel distance values (20). This method compares the grayscale-level differences between two different pixels at different locations. In recent years, several studies conducted with magnetic resonance imaging (MRI) (20) and computed tomography (21) have shown promising results using GLCM texture features for benign-malignant differentiation of lesions in bone and prostate, and for the detection of bone metastases. In a study by Yildirim et al. (22), bone mineral density (BMD) of the lumbar spine, femoral neck, and total femur determined by dual-energy X-ray absorptiometry (DXA) was compared between subjects with FMF and healthy subjects, and it was shown that BMD was lower in FMF patients. Researchers have reported that bone mass reduction may be related to the chronic inflammatory feature of the disease and chronic inflammation may affect bone turnover and metabolism. FMF is a common disease in the Turkish population and there is insufficient data in the literature regarding its effect on the trabecular and cortical structure of the jaw bones. The aim of this study was

to determine the changes in mandibular cortical morphology, trabecular bone microarchitecture, and textural properties of FMF patients compared with the healthy control group using panoramic radiographs.

Methods

Sample Selection and Study Design

The ethical approval for the study was obtained from Necmettin Erbakan University Faculty of Dentistry (decision no: 2023/257, date: 23.02.2023). The study was carried out by retrospectively collecting panoramic radiographs in the database of individuals who were admitted to the Dentomaxillofacial Radiology clinic for dental examination between 2021 and 2022 and who had a diagnosis of FMF in their medical history. All panoramic radiographs within the scope of the study were obtained with a 2D Veraviewpocs (J MORITA MFG corp, Kyoto, Japan) digital panoramic device with irradiation parameters of 70 kV, 5 mA, and 15 s. Individuals with a history of FMF constituted the case group and systemically healthy individuals who matched the case group in terms of age and gender constituted the control group.

Patients with FMF (all cases consisting of colchicine users with various dosages: 0.5-3 mg/day), and their age- and sex-matched, systemically healthy subjects aged ≥18 years with teeth were included. The presence of maxillofacial pathologies visualized on panoramic radiographs, radiographs of edentulous individuals, and panoramic radiographs that were not diagnostically adequate due to patient positioning or irradiation errors were excluded from the study.

Morphological Evaluation

The MCI scores of 100 patients (50 cases and 50 controls) were evaluated twice at 14-day intervals by the same observer (M.T.) with 11 years of experience in oral radiology. The Kappa value for intraobserver agreement was calculated as 0.94. In MCI, bone resorption in the cortical region extending from the distal foramen mentale to the antegonial region is analyzed. According to this index (11):

C1 (Normal Mandibular Cortex): The margins are equal and sharp on both sides of the cortex.

C2 (Moderately Resorbed Mandibular Cortex): The endosteal margins of the cortex show half-moon-shaped defects (lacunar resorption) and the margins are observed as 1-3 layers.

C3 (Severely Resorbed Cortex): Cortical cortices are severely porous with dense endosteal debris.

In the MCI index, panoramic radiographs are evaluated and graded separately for right and left, and then a single grade is assigned for each panoramic radiograph. In determining the final class, the class with more morphologic destruction is preferred to the class with less destruction (Figure 1).

Image Pre-processing

The panoramic radiographs saved in *.tiff format were first resized for homogeneous study (2943x1435 pixels). Then, selected ROI from the trabecular bone region between the second premolar and first molar roots were cut with the ImageJ program with equal row and column sizes (50x50 pixels) (Figure 2).

Histogram equalization was performed on 50 FMF (+) and 50 FMF (-) ROI images with 50x50 row and column sizes to increase the contrast of textural changes and to examine them at an equal pixel grayscale-level range. Histogram-equalized images were used to obtain FOS and GLCM features.

Fractal Analysis

The same regions of the case and control images were cut and the FD analysis of the trabecular bone was calculated with the ImageJ program using the box-counting technique described by White and Rudolph (23) (Figures 3, 4). Measurements were calculated by the same observer (M.T.).

First Order Statistics

The FOS is a texture feature extraction method obtained without considering the relationship in pixel neighborhoods. With the FOS feature extraction method, mean, kurtosis, variance, skewness, entropy, and energy values are calculated based on the histogram representing the frequency of the pixel distribution in the image. The histogram is a statistical definition of the number of times the pixel intensity values are repeated throughout the image. In two-dimensional space, the image size is expressed in width and height. By multiplying the width and length, the total pixel number of the ROI region can be calculated.

Gray-level Co-occurrence Matrix

While the FOS features provide simple statistical properties of grayscale-level pixel values in the image, they do not give differences due to inter-pixel neighborhoods. Therefore, high-order texture statistics, such as GLCM, can characterize textural differences due to neighborhoods between pixels. There are
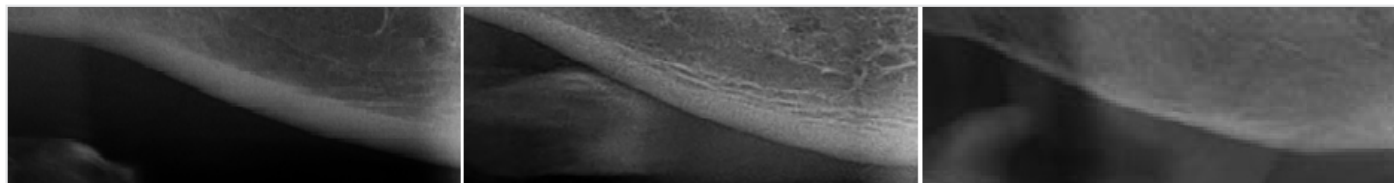
Figure 1. MCI description on cropped panoramic images (left to right: C1, C2, C3)

MCI: Mandibular cortical index

two important parameters for the GLCM method, also known as second-order texture statistics: Pixel neighborhood distance (D) and pixel neighborhood orientation degree (θ). A pixel of interest in the image has 8 neighbors. These neighborhoods consist of horizontal 0°, vertical 90°, right 45°, anti-diagonal 135° directions, and their four opposite directions in terms of degrees. Neighborhood distance is a measure of how far from the pixel of interest it is to a neighboring pixel that needs to be processed (15-17). In Figure 4, pixel values in a region of the FMF ROI obtained after histogram equalization and neighborhood orientations of a pixel of interest are given. Table 1 shows the pixel neighborhood orientation angles and offset values of the pixel distance of interest.

In this study, 19 second-order statistics were obtained by forming co-occurrence matrices from FMF (+) and FMF (-) ROI images according to four different θ angles and 1 offset value [0° (0 1), 90° (-1 0), 45° (-1 1), 135° (-1 -1)] (19,24-28). These statistics are given in Table 2.
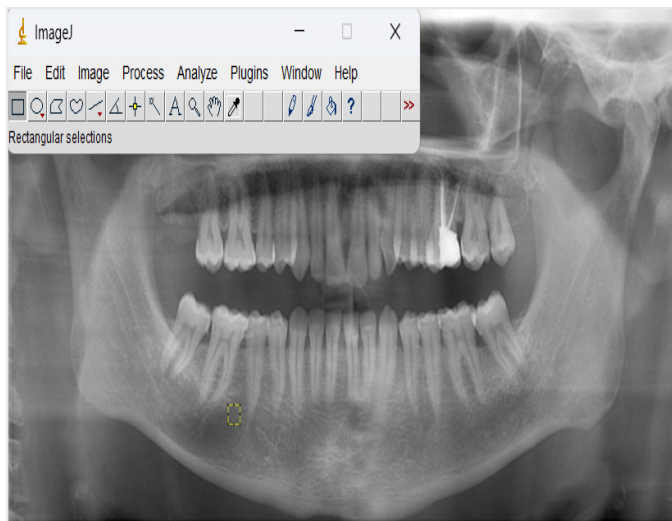
Figure 2. The selected ROI (50x50 pixel dimensions)

ROI: Regions of interest
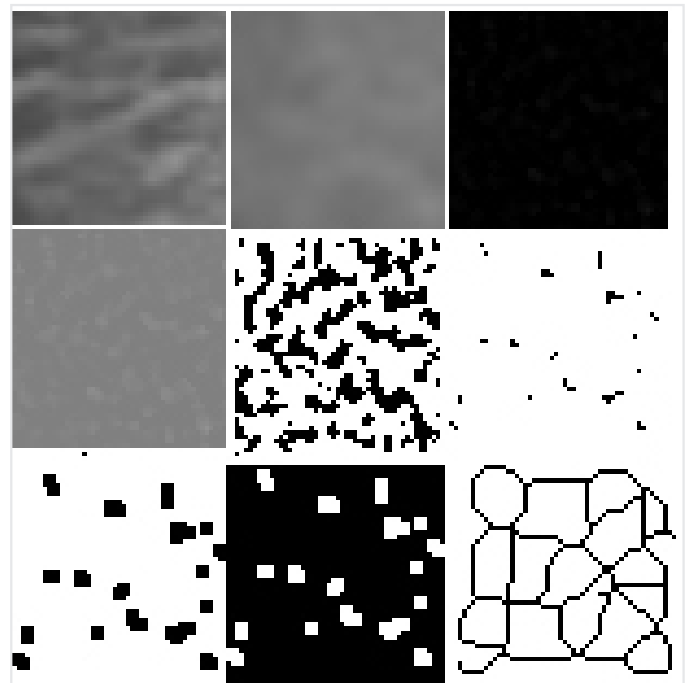
Figure 3. (a) ROI selection, (b) Gaussian filter (c) Subtraction of the ROI from the original image (d) Addition of 128 gray-scale values to each pixel location (e) Binarization (f) Erosion (g) Dilatation (h) Invertion (i) Skeletonization

ROI: Regions of interest
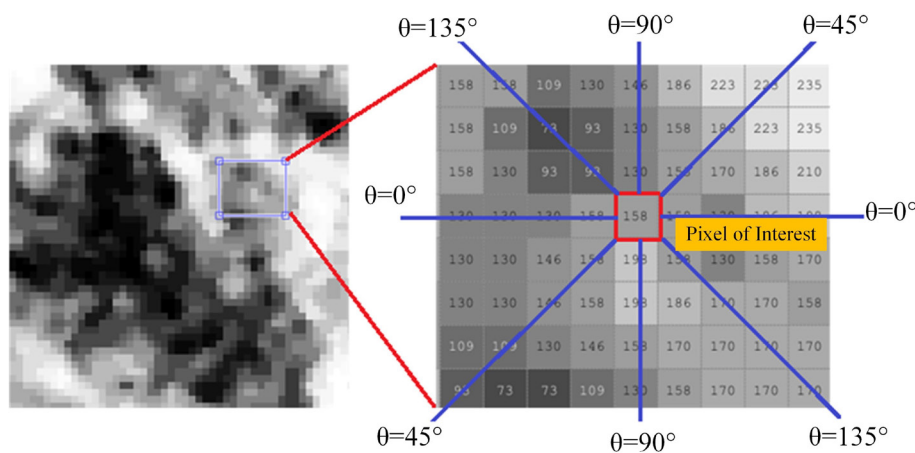
Figure 4. FMF ROI image obtained after histogram equalization, and neighborhood orientations relative to a pixel point of interest in a region within the image

FMF: Familial Mediterranean fever, ROI: Regions of interest

Table 1. Pixel neighborhood orientation angles and offset representations of the pixel distance of interest

The Orientation Angel (θ)	Offset (Distance)
0° (horizontal)	[0 D]
45° (diagonal)	[-D D]
90° (vertical)	[-D 0]
135° (anti-diagonal)	[-D -D]

Statistical Analysis

The data obtained were evaluated using SPSS v21.0 (IBM Corp, Armonk, NY, USA). The Kolmogorov-Smirnov test was used to determine the normality of data. For statistical significance between two independent groups, independent samples t-test, Mann-Whitney U test, and Spearman correlation analysis were performed. The significance between categorical data was

Table 2. Second-order features obtained with GLCM and statistical results

Features	Stats	FMF(-) (0.1)	FMF(+) (0.1)	p	FMF(-) (45.1)	FMF(+) (45.1)	p	FMF(-) (90.1)	FMF(+) (90.1)	p	FMF(-) (135.1)	FMF(+) (135.1)	p
1. autoc	Mean	25.036	24.956	0.616	24.608	24.582	0.819	24.869	24.891	0.656	24.654	24.607	0.589
	Std	0.509	0.604		0.611	0.685		0.525	0.617		0.595	0.698	
2. contr	Mean	0.841	0.931	0.753	1.620	1.663	0.618	1.105	1.108	0.711	1.529	1.617	0.409
	Std	0.391	0.408		0.619	0.677		0.372	0.417		0.565	0.652	
3.corrp	Mean	0.920	0.911	0.960	0.845	0.841	0.827	0.895	0.895	0.977	0.854	0.846	0.707
	Std	0.038	0.038		0.061	0.064		0.037	0.039		0.056	0.061	
4. cprom	Mean	723.138	711.352	0.374	672.246	664.316	0.299	704.180	698.546	0.130	676.992	666.018	0.164
	Std	43.571	34.592		49.215	38.249		41.047	29.528		49.300	36.062	
5. cshad	Mean	0.434	0.418	0.249	0.489	0.210	0.278	0.402	0.047	0.366	0.475	0.371	0.282
	Std	4.405	6.832		4.454	6.758		4.376	6.745		4.459	6.536	
6. dissi	Mean	0.554	0.585	0.936	0.843	0.844	0.414	0.665	0.654	0.542	0.819	0.835	0.452
	Std	0.150	0.159		0.176	0.209		0.126	0.148		0.170	0.202	
7. energ	Mean	0.055	0.054	0.326	0.041	0.042	0.716	0.049	0.050	0.931	0.042	0.042	0.920
	Std	0.010	0.009		0.007	0.008		0.007	0.007		0.007	0.008	
8. entro	Mean	3.165	3.196	0.444	3.455	3.443	0.803	3.296	3.277	0.919	3.433	3.437	0.930
	Std	0.196	0.189		0.172	0.193		0.153	0.161		0.168	0.179	
9. homop	Mean	0.751	0.741	0.847	0.652	0.655	0.277	0.710	0.717	0.536	0.658	0.657	0.454
	Std	0.054	0.058		0.050	0.065		0.043	0.051		0.051	0.062	
10. maxpr	Mean	0.107	0.105	0.763	0.092	0.091	0.230	0.101	0.101	0.453	0.093	0.092	0.327
	Std	0.012	0.011		0.011	0.009		0.010	0.009		0.012	0.010	
11. sosvh	Mean	25.277	25.347	0.789	25.027	25.156	0.781	25.069	25.122	0.465	25.102	25.028	0.437
	Std	0.515	0.551		0.578	0.626		0.525	0.586		0.546	0.623	
12. savgh	Mean	8.989	8.986	0.533	8.986	8.989	0.265	8.985	8.993	0.318	8.986	8.989	0.276
	Std	0.100	0.125		0.105	0.132		0.105	0.130		0.105	0.132	
13. svarh	Mean	60.290	60.050	0.988	58.991	58.931	0.860	59.686	59.782	0.861	59.094	58.985	0.956
	Std	1.673	1.743		1.707	1.788		1.586	1.686		1.699	1.821	
14. senth	Mean	2.656	2.658	0.424	2.686	2.685	0.855	2.674	2.670	0.887	2.686	2.685	0.891
	Std	0.036	0.029		0.016	0.014		0.023	0.018		0.018	0.015	
15. dvarh	Mean	0.841	0.931	0.753	1.620	1.663	0.618	1.105	1.108	0.711	1.529	1.617	0.409
	Std	0.391	0.408		0.619	0.677		0.372	0.417		0.565	0.652	
16. denth	Mean	0.933	0.970	0.887	1.191	1.191	0.331	1.049	1.043	0.360	1.171	1.185	0.468
	Std	0.164	0.176		0.151	0.187		0.128	0.155		0.146	0.176	
17. inf1h	Mean	-0.462	-0.444	0.789	-0.321	-0.324	0.391	-0.398	-0.404	0.515	-0.331	-0.327	0.608
	Std	0.090	0.094		0.078	0.098		0.069	0.083		0.076	0.091	
18. inf2h	Mean	0.916	0.909	0.966	0.847	0.845	0.800	0.893	0.894	0.951	0.854	0.848	0.744
	Std	0.032	0.033		0.053	0.056		0.031	0.034		0.049	0.054	
19. indnc	Mean	0.941	0.939	0.882	0.914	0.914	0.360	0.931	0.932	0.532	0.916	0.915	0.462
	Std	0.014	0.015		0.015	0.019		0.012	0.014		0.015	0.018	

autoc: Autocorrelation, contr: Contrast, corrp: Correlation, cprom: Cluster Prominence, cshad: Cluster Shade, dissi: Dissimilarity, energ: Energy, entro: Entropy, homop: Homogeneity, maxpr: Maximum probability, sosvh: Sum of sqaures:Variance, savgh: Sum average, senth: Sum entropy, dvarh: Difference variance, denth: Difference entropy, inf1h: Information measure of correlation1, inf2h: Information measure of correlation2, indnc: Inverse difference normalized (INN), , FMF: Familial Mediterranean fever, GLCM: Gray-level co-occurrence matrix

evaluated with chi-square test. The evaluation of the test results was made according to a 0.05 significance level.

Results

There were 54 women and 46 men in the case (n=50) and control (n=50) groups consisting of 100 individuals. The age range of the patients matched in terms of age and gender was 18-71 years with a mean age of 30±13 years. MCI scores related to the mandibular cortex did not differ significantly between the case and control groups (p>0.05) (Table 3).

The FD values for mandibular trabecular bone were 1.43 in the case group and 1.44 in the control group, and there was no significant difference between them (p>0.05). All the patients in the case group consisted of individuals using colchicine. The distribution of the individuals according to the colchicine doses they used daily is given in Table 4. There was no significant correlation between colchicine doses and FD (p>0.05).

The FOS properties and statistical values of trabecular bone are given in Table 5. There was no statistically significant difference between the case and control groups (p>0.05).

In Table 2, second-order features obtained with GLCM and statistical results are given. There was no statistically significant difference between the case and control groups (p>0.05).

Discussion

The FMF is a common disease in the Turkish population (3) and BMD has been reported to be decreased in FMF (22). Based on this, we aimed to investigate possible differences related to FMF in the jaw bones of these patients. For this purpose, MCI was used to evaluate cortical bone, FD, first and second-order image features (GLCM) were used to examine trabecular bone on panoramic images.

Fractal analysis is used to evaluate the effects of various drugs (bisphosphonate, corticosteroid, antiepileptics, aromatase inhibitor, selective serotonin reuptake inhibitors, proton pump inhibitors), systemic diseases and conditions (sickle cell anemia, thalassemia, type I and II diabetes mellitus on the jaws, osteogenesis imperfecta, chronic renal failure, osteoporosis) (29-31). In the study conducted by Bayrak et al. (29), panoramic radiographs were used, 59 patients with thalassemia major

Table 3. The distribution of the sample according to MCI scores

| | MCI (number of subjects) | | | Total | x² |
	1	2	3		
Control, n	36	13	1	50	
	72.0%	26.0%	2.0%	100.0%	
Case, n	27	21	2	50	p>0.05
	54.0%	42.0%	4.0%	100.0%	
Total, n	63	34	3	100	
	63.0%	34.0%	3.0%	100.0%	

MCI: Mandibular cortical index

Table 4. The distribution of individuals in the case group according to daily colchicine usage doses

	The number of patients	Valid percentage %
0.5 mg	11	22.0
1 mg	3	6.0
1.5 mg	25	50.0
3 mg	11	22.0
Total	50	100.0

Table 5. FOS features and statistical values

| | FMF (+) | | FMF (-) | | |
FOS	Mean	Std	Mean	Std	p-value
Mean	129.5411	0.6000	129.4133	0.6088	0.887
Variance	5396.4161	68.8685	5419.3532	55.2592	0.235
Skewness	0.0031	0.0081	0.0019	0.0073	0.534
Kurtosis	1.8050	0.0127	1.8047	0.0120	0.776
Entropy	4.3089	0.5517	4.3280	0.5402	0.882
Energy	0.0601	0.0241	0.0590	0.0232	0.653

FOS: First-order statistics, FMF: Familial Mediterranean fever

and 59 controls were included, and FD was measured in 4 separate ROIs. It was stated that FD was lower in the cases in 2 of the 4 selected ROIs, and there was no significant difference between cases and controls in the other 2 ROIs. In their study investigating lactation-induced bone loss, Coşgunarslan et al. (31) selected 3 different ROIs, including cortical and trabecular bone, on panoramic radiographs. While FD was significantly lower in the case group in the 1st and 2nd ROIs selected from the trabecular bone, no difference was found between the case andcontrol groups in the ROI selected from the cortical bone. Based on the findings of these studies, it appears that selecting different ROIs may affect the results.

In the medical field, GLCM textural features can be used for brain tumor classification using MRI images (32), brain cancer diagnosis using histopathological images (33), malignant-benign differentiation of liver tumors using US images (34), classification (35) and early detection of benign-malignant breast masses using mammography images (36), skin tissue analysis for allergic, viral, bacterial and fungal skin diseases (37). It has been used in many fields such as examination of changes in the parotid gland after radiotherapy using the ultrasound (US) (38), prostate cancer classification using prostate biopsy sections (39), early diagnosis of lung cancer using computed tomography (CT) images (40), diagnosis of skin melanomas using dermoscopy images (41), diagnosis of esophageal cancer using positron emission tomography images images (42), benign-malignant differentiation of thyroid nodules using US images (43), detection of cervical cancer using colposcopy images (44) and many others. GLCM textural feature studies in the field of dentistry are very limited. In the study by Kavitha et al. (45) mandibular cortical width and GLCM features were calculated on panoramic radiographs for the detection of osteoporosis in Korean women. They reported that the use of all three together instead of a single feature had higher accuracy in the diagnosis of osteoporosis. Another study (46) showed that GLCM features were successful in detection of caries in intraoral images. Veena et al. (47) examined GLCM features (entropy, contrast, homogeneity, energy, and correlation) in terms of dental caries and cysts using panoramic radiographs and reported that these features might be helpful in diagnosis.

Various studies are investigating a more economical solution by examining textural features instead of DXA, which is the traditional method for evaluating bone quality related to osteoporosis. Kawashima et al. (48) used GLCM texture analysis for the detection of osteoporosis on non-contrast head CTs. It was shown that many regions in the skull base and maxillofacial bones had different GLCM texture characteristics between individuals with normal BMD and patients with osteoporosis. They stated that quantitative analysis of the microarchitecture in cancellous bone on non-contrast head CT images could be used as a new indicator in the diagnosis of osteoporosis. In another study (49) femur radiographs were used for texture analyses. It was concluded that tissue information contained in the trabecular bone structure visualized on radiographs could predict whether an implant anchor could be used and determine local bone quality from preoperative radiographs. The lack of textural difference between the case and control groups in the current study may be related to the imaging method used and the selected mandibular trabecular bone structure being different from other studies.

In the study by Hwang et al. (50) the diagnosis of osteoporosis was investigated by calculating FD and GLCM values on panoramic radiographs. Four different ROIs were selected and it was reported that the ROI selected from the mandibular cortex showed more strut features (quantification of the structural elements of the bone) than the medullary bone in the comparison of patients with and without osteoporosis. While individuals with osteoporosis showed lower FD in the ROI region selected from the endosteal region of the bone, no difference in FD was observed between the two groups in the trabecular bone region. In the present study, no significant difference related to FMF was found in the ROI selected from the medullary bone in FD and GLCM calculation. The only study in the literature on FMF in which FD was calculated from panoramic radiographs was conducted with pediatric patients aged 5-15 years. In this study (30) there was no difference in FD and MCI between healthy and FMF children. In addition, there was no correlation between the duration of colchicine use (in months) and FD. The findings of the present study were similar. FD and MCI were similar in adults with FMF and healthy individuals. There was no significant correlation between the dose (mg) of colchicine used and FD. FMF did not affect FD values and MCI of mandibular trabecular bone.

MCI has well-defined cut-off values, as the score from C1 to C3 increases, the porosity of the endosteal margin of the cortex increases. In the literature, the results of studies on MCI are conflicting. MCI was recommended as a feasible tool to screen initial BMD loss (osteopenia). The sensitivity and specificity of MCI for osteopenia were 0.81 and 0.48, respectively. The sensitivity and specificity of MCI for osteoporosis were, 0.35 and 0.88, respectively (51). Conversely, the findings of the present study showed that there was no difference in terms of MCI scores between FMF cases and controls. Similar to our results, Pacheco-Pereira et al. (52) revealed that MCI did not differ between patients with familial adenomatous polyposis and the control group and FD values were lower in the cases. They concluded that MCI was not useful for the analysis of the cortical bone pattern and FD was a promising tool for bone structure evaluation in dental panoramic radiographs. The age and gender distributions of the samples examined in the studies may affect the results obtained. Additionally, all individuals examined in this study used colchicine. It has been reported that colchicine inhibits bone resorption by reducing the number of osteoclasts and thus prevents osteoporosis (53). Accordingly, MCI values may not have differed between FMF case and control groups.

In the study conducted by Yildirim et al. (22), lumbar and femoral BMD values were found to be significantly lower in individuals with FMF than in healthy individuals, as a result of measurements made with DXA. In the mentioned study, 28

patients with FMF and 30 controls were evaluated. The mean age of the sample was older than the present study (35.1 for patients and 36.6 for controls). Contrary to this study, no difference was found between patients with FMF and healthy individuals in our examinations. It should be taken into consideration that the measurements were performed in the mandible, which was a different region, and the medullary structure of the femoral and lumbar bones might be different compared to the mandible. Additionally, the age and gender distribution of the sample might have an impact on differences in results.

Study Limitations

With its anti-inflammatory, anti-oxidative, anti-apoptotic, and bone-protective effects, colchicine treatment has been reported to have a prophylactic effect in preventing alveolar bone loss (54). These positive effects of colchicine in individuals with FMF might be the reason why there was no difference in FD and GLCM values between the case and control groups in this study. A limitation of the present study was that it was a retrospective study and there might be other possible systemic diseases of the individuals that were not yet diagnosed. Although the number of patients examined in this study was limited due to the relatively low number of patients receiving regular FMF treatment in adulthood, this study was planned to be improved with the inclusion of new patients.

Conclusion

Morphologic features of the mandibular cortex and fractal and textural features of the trabecular bone did not show a difference on panoramic radiographs between FMF patients and healthy controls. Further studies with different imaging techniques and image processing methods are needed.

Ethics

Ethics Committee Approval: The ethical approval for the study was obtained from Necmettin Erbakan University Faculty of Dentistry (decision no: 2023/257, date: 23.02.2023).

Informed Consent: Retrospective study.

Authorship Contributions

Concept: M.T., M.Ü.Ö., Design: M.T., M.Ü.Ö., Data Collection or Processing: M.T., M.Ü.Ö., Analysis or Interpretation: M.T., M.Ü.Ö., Literature Search: M.T., M.Ü.Ö., B.Ö., Writing: M.T., M.Ü.Ö., B.Ö.

Conflict of Interest: No conflict of interest was declared by the authors.

Financial Disclosure: The authors declared that this study received no financial support.

References

1. Ozen S, Batu ED. The myths we believed in familial Mediterranean fever: what have we learned in the past years? Semin Immunopathol 2015;37:363-9.

2. Zadeh N, Getzug T, Grody WW. Diagnosis and management of familial Mediterranean fever: integrating medical genetics in a dedicated interdisciplinary clinic. Genet Med 2011;13:263-9.

3. Basaran O, Uncu N, Celikel BA, Aydın F, Cakar N. Assessment of neutrophil to lymphocyte ratio and mean platelet volume in pediatric familial Mediterranean fever patients. J Res Med Sci 2017;22:35.

4. Kastner DL. Familial Mediterranean fever: the genetics of inflammation. Hosp Pract (1995) 1998;33:131-4, 139-40, 143-6 passim.

5. Cantarini L, Rigante D, Brizi MG, Lucherini OM, Sebastiani GD, Vitale A, et al. Clinical and biochemical landmarks in systemic autoinflammatory diseases. Ann Med 2012;44:664-73.

6. Bostancı V, Toker H, Senel S, Sahin S. Prevalence of periodontal disease in patients with Familial Mediterranean Fever: a cohort study from central Türkiye. Quintessence Int 2014;45:743-8.

7. Aypar E, Ozen S, Okur H, Kutluk T, Besbas N, Bakkaloglu A. Th1 polarization in familial Mediterranean fever. J Rheumatol 2003;30:2011-3.

8. Esmeray P, Keçeli Tİ, Tekçiçek M, Batu ED, Arıcı ZS, Ünlü HK, et al. Oral health status in children with familial Mediterranean fever. Turk J Pediatr 2021;63:443-9.

9. Ak KB, Suzen M, Uçkan S. Aseptic Arthritis of the Temporomandibular Joint with Severe Inflammation in an FMF Patient: A Case Report. Journal of Anatolian Medical Research 2022;7:35-40.

10. Kwon AY, Huh KH, Yi WJ, Lee SS, Choi SC, Heo MS. Is the panoramic mandibular index useful for bone quality evaluation? Imaging Sci Dent 2017;47:87-92.

11. Klemetti E, Kolmakov S, Kröger H. Pantomography in assessment of the osteoporosis risk group. Scand J Dent Res 1994;102:68-72.

12. Güleç M, Taşsöker M, Şener S. Tıpta ve Diş Hekimliğinde Fraktal Analiz. Ege Üniversitesi Diş Hekimliği Fakültesi Dergisi 2019;40:17-31.

13. Demirhan A, Güler İ. Image Segmentatıon Usıng Self-Organızıng Maps And Gray Level Co-Occurrence Matrıces. J. Fac. Eng. Arch. Gazi Univ 2010;25:285-91.

14. Aggarwal N, Agrawal R. First and second order statistics features for classification of magnetic resonance brain images. Journal of Signal and Information Processing 2012.

15. Yusof NSM, Dewi DEO, Faudzi AAM, Salih NM, Bakar NA, Hamid HA. Ultrasound imaging characterization on tissue mimicking materials for cardiac tissue phantom: Texture analysis perspective. Malaysian Journal of Fundamental and Applied Sciences 2017;17:4-2.

16. Cai JH, He Y, Zhong XL, Lei H, Wang F, Luo GH, et al. Magnetic Resonance Texture Analysis in Alzheimer's disease. Acad Radiol 2020;27:1774-83.

17. Parekh V, Jacobs MA. Radiomics: a new application from established techniques. Expert Rev Precis Med Drug Dev 2016;1:207-26.

18. Materka A, Strzelecki M. Texture analysis methods-a review. Technical university of lodz, institute of electronics, COST B11 report, Brussels 1998;10:4968.

19. Haralick RM, Shanmugam K, Dinstein I. Textural Features for Image Classification. IEEE Transactions on Systems, Man, and Cybernetics 1973;SMC-3:610-21.

20. Wang Y, Yu B, Zhong F, Guo Q, Li K, Hou Y, et al. MRI-based texture analysis of the primary tumor for pre-treatment prediction of bone metastases in prostate cancer. Magn Reson Imaging 2019;60:76-84.

21. Suhas M, Swathi B. Significance of haralick features in bone tumor classification using support vector machine. Paper presented at: Engineering Vibration, Communication and Information Processing: ICoEVCI 2018, India2019.

22. Yildirim K, Karatay S, Cetinkaya R, Uzkeser H, Erdal A, Capoglu I, et al. Bone mineral density in patients with familial Mediterranean fever. Rheumatol Int 2010;30:305-8.

23. White SC, Rudolph DJ. Alterations of the trabecular pattern of the jaws in patients with osteoporosis. Oral Surg Oral Med Oral Pathol Oral Radiol Endod 1999;88:628-35.

24. Soh L-K, Tsatsoulis C. Texture analysis of SAR sea ice imagery using gray level co-occurrence matrices. IEEE Transactions on geoscience and remote sensing. 1999;37:780-95.

25. Brynolfsson P, Nilsson D, Torheim T, Asklund T, Karlsson CT, Trygg J, et al. Haralick texture features from apparent diffusion coefficient (ADC) MRI images depend on imaging and pre-processing parameters. Sci Rep 2017;7:4041.

26. Löfstedt T, Brynolfsson P, Asklund T, Nyholm T, Garpebring A. Gray-level invariant Haralick texture features. PloS one 2019;14:e0212110.

27. Clausi DA. An analysis of co-occurrence texture statistics as a function of grey level quantization. Canadian Journal of remote sensing 2002;28:45-62.

28. Uppuluri A. GLCM texture features MATLAB Central File Exchange 2023; https://www.mathworks.com/matlabcentral/fileexchange/22187-glcm-texture-features. Accessed Retrieved June 24, 2023.

29. Bayrak S, Göller Bulut D, Orhan K, Sinanoğlu EA, Kurşun Çakmak EŞ, Mısırlı M, et al. Evaluation of osseous changes in dental panoramic radiography of thalassemia patients using mandibular indexes and fractal size analysis. Oral Radiol 2020;36:18-24.

30. Altunok Ünlü N, Coşgun A, Altan H. Evaluation of bone changes on dental panoramic radiography using mandibular indexes and fractal dimension analysis in children with familial Mediterranean fever. Oral Radiol 2023;39:312-20.

31. Coşgunarslan A, Canger EM, Soydan Çabuk D, Kış HC. The evaluation of the mandibular bone structure changes related to lactation with fractal analysis. Oral Radiol 2020;36:238-47.

32. Zulpe N, Pawar V. GLCM textural features for brain tumor classification. International Journal of Computer Science Issues (IJCSI) 2012;9:354-59.

33. Durgamahanthi V, Anita Christaline J, Shirly Edward A. GLCM and GLRLM Based Texture Analysis: Application to Brain Cancer Diagnosis Using Histopathology Images. Intelligent Computing and Applications, Proceedings of ICICA 2019 2020:691-706.

34. Xian G-m. An identification method of malignant and benign liver tumors from ultrasonography based on GLCM texture features

and fuzzy SVM. Expert Systems with Applications 2010;37:6737-41.

35. Mohanty AK, Beberta S, Lenka SK. Classifying benign and malignant mass using GLCM and GLRLM based texture features from mammogram. International Journal of Engineering Research and Applications 2011;1:687-93.

36. Htay TT, Maung SS. Early stage breast cancer detection system using glcm feature extraction and k-nearest neighbor (k-NN) on mammography image. 2018 18th International Symposium on Communications and Information Technologies (ISCIT) 2018.

37. Arabi PM, Joshi G, Vamsha Deepa N. Performance evaluation of GLCM and pixel intensity matrix for skin texture analysis. Perspectives in Science 2016;8:203-6.

38. Yang X, Tridandapani S, Beitler JJ, Yu DS, Yoshida EJ, Curran WJ, et al. Ultrasound GLCM texture analysis of radiation-induced parotid-gland injury in head-and-neck cancer radiotherapy: an in vivo study of late toxicity. Med Phys 2012;39:5732-9.

39. Tahir MA, Bouridane A, Kurugollu F. An FPGA Based Coprocessor for GLCM and Haralick Texture Features and their Application in Prostate Cancer Classification. Analog Integrated Circuits and Signal Processing 2005;43:205-15.

40. Althubiti SA, Paul S, Mohanty R, Mohanty SN, Alenezi F, Polat K. Ensemble Learning Framework with GLCM Texture Extraction for Early Detection of Lung Cancer on CT Images. Comput Math Methods Med 2022;2022:2733965.

41. Sheha MA, Mabrouk MS, Sharawy A. Automatic detection of melanoma skin cancer using texture analysis. International Journal of Computer Applications 2012;42:22-6.

42. Doumou G, Siddique M, Tsoumpas C, Goh V, Cook GJ. The precision of textural analysis in 18F-FDG-PET scans of oesophageal cancer. European Radiology 2015;25:2805-12.

43. Song G, Xue F, Zhang C. A Model Using Texture Features to Differentiate the Nature of Thyroid Nodules on Sonography. Journal of Ultrasound in Medicine 2015;34:1753-60.

44. Novitasari DCR, Asyhar AH, Thohir M, Arifin AZ, Mu'jizah H, Foeady AZ. Cervical Cancer Identification Based Texture Analysis Using GLCM-KELM on Colposcopy Data. 2020 International Conference on Artificial Intelligence in Information and Communication (ICAIIC). 2020.

45. Kavitha MS, An SY, An CH, Huh KH, Yi WJ, Heo MS, et al. Texture analysis of mandibular cortical bone on digital dental panoramic radiographs for the diagnosis of osteoporosis in Korean women. Oral Surg Oral Med Oral Pathol Oral Radiol 2015;119:346-56.

46. Geetha V, Aprameya K. Textural analysis based classification of digital X-ray images for dental caries diagnosis. Int J Eng Manuf (IJEM) 2019;9:44-5.

47. Veena DK, Jatti A, Joshi R, Deepu KS. Characterization of dental pathologies using digital panoramic X-ray images based on texture analysis. Annu Int Conf IEEE Eng Med Biol Soc 2017;2017:592-5.

48. Kawashima Y, Fujita A, Buch K, Li B, Qureshi MM, Chapman MN, et al. Using texture analysis of head CT images to differentiate

osteoporosis from normal bone density. Eur J Radiol 2019;116:212-8.

49. Huber MB, Carballido-Gamio J, Fritscher K, Schubert R, Haenni M, Hengg C, et al. Development and testing of texture discriminators for the analysis of trabecular bone in proximal femur radiographs. Med Phys 2009;36:5089-98.

50. Hwang JJ, Lee JH, Han SS, Kim YH, Jeong HG, Choi YJ, et al. Strut analysis for osteoporosis detection model using dental panoramic radiography. Dentomaxillofac Radiol 2017;46:20170006.

51. Kinalski MA, Boscato N, Damian MF. The accuracy of panoramic radiography as a screening of bone mineral density in women: a systematic review. Dentomaxillofac Radiol 2020;49:20190149.

52. Pacheco-Pereira C, Silvestre-Barbosa Y, Almeida FT, Geha H, Leite AF, Guerra ENS. Trabecular and cortical mandibular bone investigation in familial adenomatous polyposis patients. Sci Rep 2021;11:9143.

53. Ersan N, Özel B. Fractal dimension analysis of different mandibular regions in familial Mediterranean fever patients: A cross-sectional retrospective study. PLoS One 2023;18:e0288170.

54. Aral CA, Aral K, Yay A, Özçoban Ö, Berdeli A, Saraymen R. Effects of colchicine on gingival inflammation, apoptosis, and alveolar bone loss in experimental periodontitis. J Periodontol 2018;89:577-85.